A Journal of the Gesellschaft Deutscher Chemiker
Angewandte Chemie
GDCh
International Edition
www.angewandte.org

Accepted Article

Title: Remote Perfluoroalkyl Substituents are Key to Living Aqueous Ethylene Polymerization

Authors: Manuel Schnitte, Janine Sophie Scholliers, Kai Riedmiller, and Stefan Mecking

To be cited as: *Angew. Chem. Int. Ed.* 10.1002/anie.201913117
Angew. Chem. 10.1002/ange.201913117

Link to VoR: http://dx.doi.org/10.1002/anie.201913117
http://dx.doi.org/10.1002/ange.201913117

WILEY-VCH

Remote Perfluoroalkyl Substituents are Key to Living Aqueous Ethylene Polymerization

Manuel Schnitte[a], Janine S. Scholliers[a], Kai Riedmiller[a], and Stefan Mecking*[a]

Abstract: Perfluoroalkyl groups are well established substituents to enhance the solubility of molecular catalysts in apolar and fluorous media. However, they have been little studied to control the catalytic properties of active sites. In various nickel(II) salicylaldiminato ethylene polymerization catalysts, which are a versatile mechanistic probe for substituent effects, longer perfluoroalkyl groups exert a strong effect on catalytic activities and polymer microstructures compared to trifluoromethyl groups as a reference. This can be accounted for by a reduced electron density on the active sites, also supported by electrochemical studies. Hereby β-hydride elimination as the key step of chain transfer and branching pathways is disfavored while chain growth rates are enhanced. This occurs to an extent that enables living polymerizations in aqueous systems to afford ultra high-molecular-weight polyethylene for various chelating salicylaldimine motifs. These findings on a mechanistically instructive as well as practically useful probe illustrates the potential of perfluoroalkyl groups for catalyst design beyond solubility, which benefits from the synthetic accessibility and stability of these electron-withdrawing groups.

Introduction

The properties of molecular catalysts are often controlled by substituents chosen to the purpose. Perfluorinated alkyls –$(CF_2)_nCF_3$ – are well-established groups to adjust the solubility of homogeneous catalysts.[1] They can enhance catalysts' lipophilicity and allow for reactions under very apolar conditions or with very apolar substrates. This enables e.g. catalysis in supercritical carbon dioxide as an alternative and an environmentally friendly solvent[2], applications in biphasic mixtures for efficient catalyst recovery[3] or selective reagent separation[4], and catalyst heterogenization and new delivery methods.[5] Strategies to make a catalyst 'fluorous' are versatile and perfluorinated groups can also be placed in the structure of a catalyst precursor to enhance its activation and reactivity via its miscibility in different phases.[6] Fluorous catalysts in general show a versatile solubility behavior and are not limited to applications in equally fluorous solvents, that are often not desired due to their costs and environmental persistence.[7]

In contrast to their extensive utilization for solubility, examples where perfluorinated alkyl groups control the active metal center's catalytic reactivity are rare.[8] Although their synthetic chemistry is well established their potential is largely unexplored in this regard.

We now report a case study showing how perfluoroalkyl substituents enhance catalyst performance. As a catalyst system, which is both mechanistically instructive to unravel the role of the perfluoroalkyl substituents as well as practically useful neutral Ni(II) polymerization catalysts were studied.[9]

Results and Discussion

Perfluoroalkyl (e.g. *n*-C_6F_{13}) substituted *N*-terphenyl salicylaldiminato Ni(II) catalysts (Figure 1) were recently demonstrated to be uniquely capable of a truly living polymerization of ethylene under aqueous conditions.[10] In this process narrow distributed ultra high-molecular-weight strictly linear polyethylene (UHMWPE) is generated, in the unusual form of monodisperse uniform-shape nanocrystals.

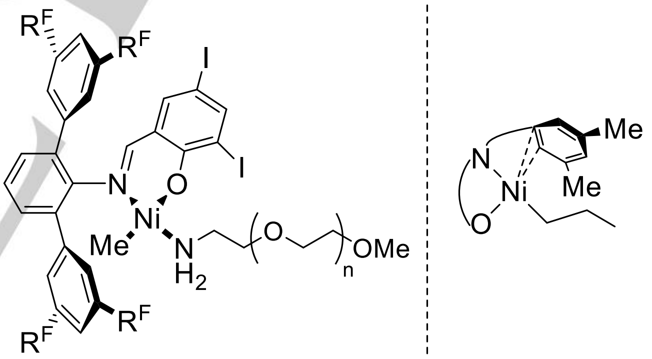

Figure 1. Catalyst precursor with C_6F_{13}-substituents in remote positions capable of truly living ethylene polymerization in aqueous media (left).[10] Interaction promoting chain transfer and branch formation in the case of electron-donating substituents, exemplified by methyl substituents (right).[11]

The strong influence of substituents in these remote positions of the chelating ligand, distant from the active center, can be related to a weak interaction between the distal aryl rings and the metal atom (Figure 1, right), that promotes decoordination of ethylene and favors β-hydride elimination (BHE).[11] BHE is the key step in chain transfer and branch formation. This weak interaction is promoted by electron-donating groups, which afford hyperbranched ethylene oligomers. In contrast, with electron-withdrawing trifluoromethyl groups linear polyethylene is formed under otherwise identical conditions.[12,13] Note that a H-F interaction with the growing chain, what has been suggested for early[14] and late transition metal catalysts[15], is clearly not operative.[16]

---

[a] Manuel Schnitte, Janine S. Scholliers, Kai Riedmiller, Prof. Dr. Stefan Mecking
Chair of Chemical Materials Science, Department of Chemistry
University of Konstanz
D-78457 Konstanz, Germany
E-mail: stefan.mecking@uni-konstanz.de

Supporting information for this article is given via a link at the end of the document.

10.1002/anie.201913117

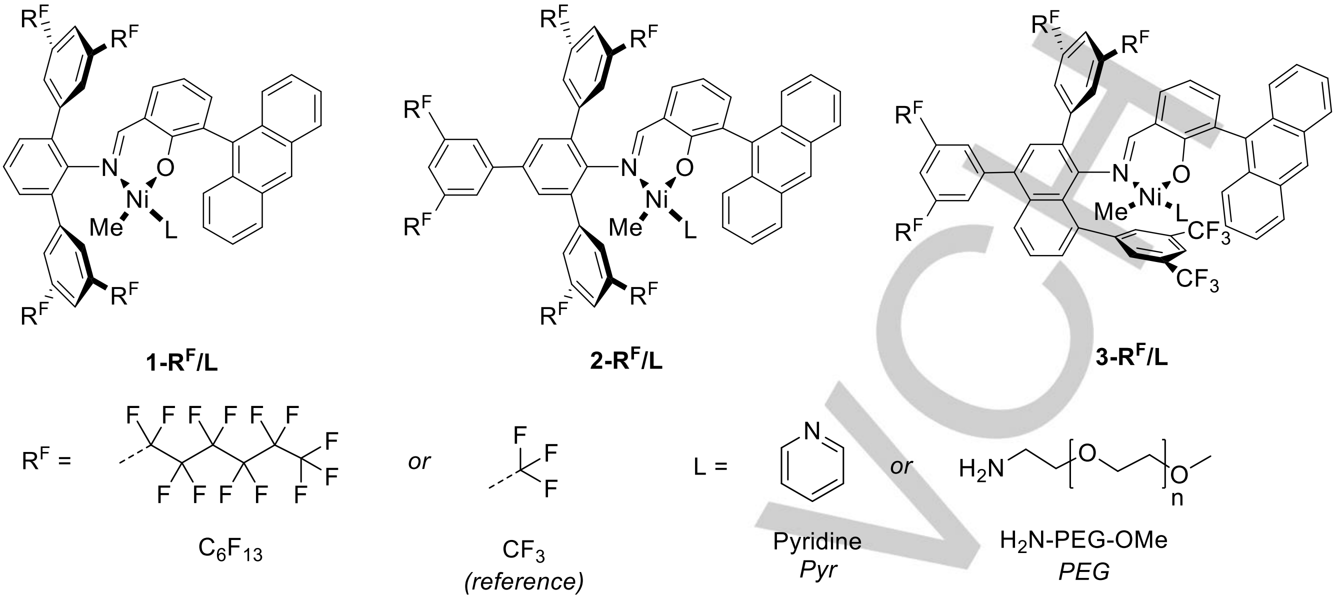

Figure 2. Catalyst precursors studied in this work. Compared to the reference systems ($R^F = CF_3$), the novel catalysts are substituted with linear long perfluoroalkyl groups ($R^F = C_6F_{13}$) in remote positions. The coordinated labile ligand L differs for lipophilic precursors (L = Pyr) and hydrophilic precursors (L = PEG), suitable for aqueous polymerizations.

To understand their role in catalysis, we investigated the influence of long perfluoroalkyl substituents (linear C_6F_{13} groups) in different established salicylaldiminato Ni(II) motifs under a set of conditions. We targeted the *N*-(quar)terphenyl based types **1/R^F-L** and **2/R^F-L** (cf. Figure 2), known to be active in aqueous and non-aqueous ethylene polymerization towards linear high-molecular-weight polyethylene.[13,17–19] We also modified *N*-naphthyl type catalyst **3/R^F-L** (cf. Figure 2), capable of a controlled/living ethylene polymerization in a variety of solvents, and introduced C_6F_{13}-substituents in selected positions.[20] Anthryl moieties were placed in close proximity to the nickel center to shield the axial site and impede chain transfer reactions.[13,21]

The synthesis of the respective salicylaldimines was straightforward according to known procedures, slightly modified to handle the highly lipophilic intermediate products (cf. the Supporting Information, SI, for details of synthesis and characterization of all catalyst precursors). As a key step, a copper-promoted Ullmann coupling of 1,3-diiodobenzene and perflurorohexyl iodide provided access to the 1,3-(diperfluorohexyl)phenyl structure motif incorporated in the aforementioned catalyst structures. Lipophilic precatalysts were obtained by reaction of salicylaldimines with [(tmeda)NiMe$_2$] in the presence of pyridine as labile ligand. Hydrophilic analogs, suitable for aqueous polymerizations, were obtained in the presence of α-methoxy-ω-amino poly(ethylene glycol) (H$_2$N-PEG-OMe, cf. Figure 2).

Ethylene polymerization studies in heptane were carried out at different temperatures (30-50 °C), with C_6F_{13}-substituted catalyst precursors and the analogous CF_3 complexes to identify effects of perfluoroalkyl substituent under lipophilic conditions (Table 1). All catalysts studied were active in ethylene polymerization and a significant effect of perfluoroalkyl chain length on catalytic performance and polymer properties was observed. Compared to their CF_3 analogues, the C_6F_{13}-substitued catalysts **1-C$_6$F$_{13}$/Pyr** and **2-C$_6$F$_{13}$/Pyr** showed higher activities (15×10^3 TO h^{-1} vs. 35×10^3 TO h^{-1}, entries 1 and 2, Table 1) and produced narrower distributed polyethylene of higher molecular weights (167×10^3 g mol^{-1} vs. 504 g mol^{-1}, entries 1 and 2, Table 1) with less branches (2.3 vs. < 1.0 branches per 1000 carbon atoms, entries 1 and 2, Table 1) at 30 °C reaction temperature. Chain transfer (which limits molecular weight and broadens molecular weight distribution) and branch formation proceed through BHE. The above data indicates a very effective suppression of these pathways by the C_6F_{13}-substitution. Similar trends of activity and branching were observed at a higher reaction temperature of 50 °C comparing CF_3- and C_6F_{13}-substitued catalyst types **1-R^F/Pyr** and **2-R^F/Pyr.**

In case of catalyst type **3-R^F/Pyr**, the C_6F_{13}-substituted derivative again produced polyethylene with lower branches. Other than this, no significant differences were observed. Both catalysts perform a highly controlled polymerization as indicated by chains per nickel ratios close to unity and narrow molecular weight distributions of $M_w/M_n = 1.2$.

The observed increase in polymerization rate and molecular weights vs. the CF_3 reference, together with a decrease in branching indicate a significant influence of the perfluoroalkyl substituents in remote positions of the catalyst structures on the active nickel center. To further illuminate the origin of this effect, cyclic voltammetry experiments were performed on all pyridine precatalysts. The observed oxidation and reduction transitions for the Ni(II)/Ni(III) pair showed that, compared to the reference trifluoromethyl catalysts, the electron density at the metal center is significantly lower in the C_6F_{13}-substituted complexes as

Table 1. Ethylene polymerization experiments in heptane.

entry	precatalyst	E_1[a] [mV]	T [°C]	yield PE [g]	TOF[b]	M_n[c] [10^3 g mol^{-1}]	M_w / M_n[c]	chains/ [Ni]	T_m[d] [°C] (Cryst. [%])	Branches /1000 C[e]
1	1-CF_3/Pyr	254	30	0.68	14.6	167	1.9	0.8	134 (53)	2.3
2	1-C_6F_{13}/Pyr	560	30	1.66	35.3	504	1.6	0.7	133 (49)	< 1.0
3	1-CF_3/Pyr	254	50	2.28	48.8	80	3.3	5.7	124 (47)	12.4
4	1-C_6F_{13}/Pyr	560	50	5.68	121.4	82	2.9	13.8	124 (50)	8.4
5	2-CF_3/Pyr	329	30	0.99	21.2	91	2.4	2.2	136 (57)	4.7
6	2-C_6F_{13}/Pyr	445	30	1.33	28.4	294	1.6	0.9	133 (55)	2.9
7	2-CF_3/Pyr	329	50	2.68	57.3	82	4.6	6.6	125 (51)	17.8
8	2-C_6F_{13}/Pyr	445	50	5.23	111.8	77	2.5	13.6	123 (49)	13.4
9	3-CF_3/Pyr	357	50	1.40	50.0	618	1.2	0.8	135 (47)	3.7
10	3-C_6F_{13}/Pyr	395	50	1.24	44.2	683	1.2	0.6	135 (46)	< 1.0

cond.: 5 µmol catalyst loading, 20 minutes reaction time, 40 bar ethylene pressure, in 100 mL heptane. [a] determined via cyclic voltammetry. [b] given in 10^3 x mol [C_2H_4] x mol^{-1} [Ni] x h^{-1}. [c] determined via GPC at 160 °C. [d] determined via DSC (heating rate: 10 K/min), 2nd heating cycle reported. [e] determined via selective detection of methyl and methylene IR-bands during GPC measurements (versus standards with known degree of branching).

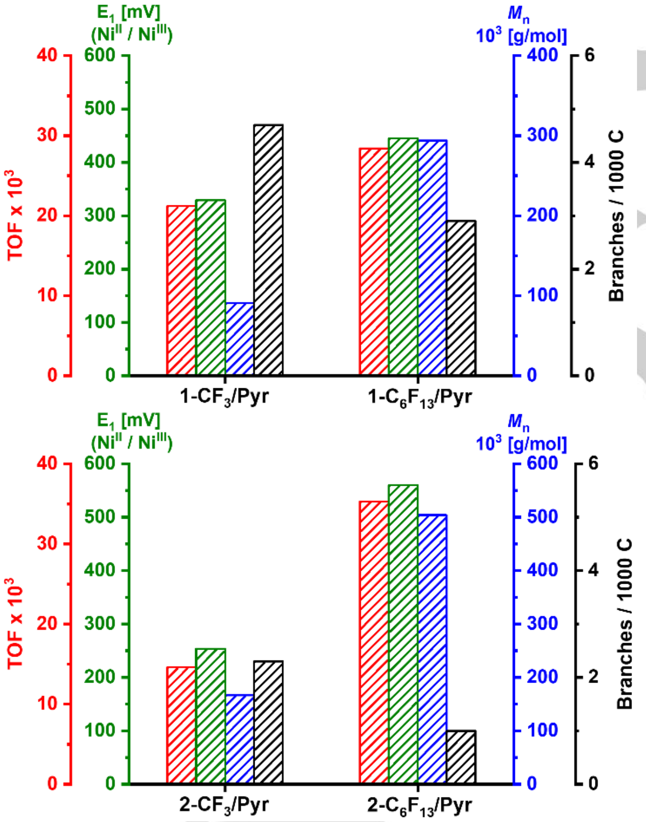

Figure 3. Comparison of experimental polymerization data with cylic voltammetry data for different catalyst precursors (**1-R^F/Pyr**, top and **2-R^F/Pyr,** bottom). Catalytic activity (TOF, red line), forward peak potential determined via cyclic voltammetry (E_1, green line), molecular weight (blue line) and branching values (black line) of polyethylenes formed versus different catalyst precursors given. Experimental data from experiments at 30 °C in heptane (entries 1, 2, 5, and 6, Table 1).

evidenced by an increase in measured forward peak potentials (column E_1, Table 1) found for all catalyst types studied. This remarkable decrease in electron density (e.g. 211 mV [$R^F = CF_3$] vs. 541 mV [$R^F = C_6F_{13}$], catalyst **1-R^F/Pyr**, Table 1) correlates qualitatively with the observed catalytic and polymer properties in case of catalyst types **1-R^F/Pyr** and **2-R^F/Pyr** (cf. Figure 3). Note, that this effect on polymer microstructure may be enhanced further by the higher steric demand[22] of perfluoroalkyl vs. trifluoromethyl substituents.

In case of catalyst types **3-R^F/Pyr**, only a small difference in forward peak potentials was observed (357 mV [$R^F = CF_3$] vs. 395 mV [$R^F = C_6F_{13}$], entries 9 and 10, Table 1). This lower effect of the substitution pattern compared to the other two types of catalysts is expected, given that only one of the aryl substituents in *o*-position of the *N*-phenyl is altered, and the phenyl ring closest to the nickel center (8-position of the naphthylamine moiety, cf. Figure 2) was not modified. This electrochemical data agrees well with the similar catalytic properties observed for **3-C_6F_{13}/Pyr** and **3-CF_3/Pyr** (Table 1), the C_6F_{13}-substitution lead to a slight decrease in branching only while catalytic activity and molecular weight are similar to the CF_3 analog.

To probe for any pronounced solvent effects, e.g. through interactions with the active site or via the solvent quality for the polymer product formed, we performed polymerization experiments in toluene as a somewhat more polar and aromatic solvent (cf. the SI for comprehensive experimental and analytical data of polymerization experiments in toluene with all catalyst precursors at different temperatures). In summary, we observed the same trends for catalysts **1-R^F/Pyr** and **2-R^F/Pyr** as outlined above with a superior role of catalysts with long perfluoroalkyl substituents. Namely, compared to the CF_3 reference (1) increased molecular weights (240 x 10^3 g mol^{-1} vs. 623 x 10^3 g mol^{-1}, entries 1 and 2, Table S1); (2) slightly increased catalytic

Table 2. Ethylene polymerization experiments in aqueous surfactant solution.

entry	precatalyst	yield PE [g]	TON[a]	M_n[b] [10^3 g mol^{-1}]	M_w / M_n[b]	chains/ [Ni]	T_m[c] [°C] (Cryst. [%])	Branches /1000 C[d]	d_h (Vol.)[e] [nm]
1	1-CF$_3$/PEG	5.87	27.9	484	2.0	1.6	142 (55) / 135 (36) 134	1.6	22 (0.05)
2	1-C$_6$F$_{13}$/PEG	9.61	45.7	866	1.3	1.5	143 (73) / 135 (48) 133	< 1.0	25 (0.08)
3	2-CF$_3$/PEG	4.78	22.7	408	1.8	1.6	140 (66) / 135 (49) 134	< 1.0	23 (0.07)
4	2-C$_6$F$_{13}$/PEG	10.65	50.6	885	1.4	1.6	140 (64) / 133 (41) 133	< 1.0	31 (0.12)
5	3-CF$_3$/PEG	1.64	7.8	486	1.6	0.5	138 (63) / 135 (51) 134	2.6	16 (0.14)
6	3-C$_6$F$_{13}$/PEG	9.39	44.6	1609	1.2	0.8	142 (65) / 136 (41) 137	< 1.0	21 (0.17)

cond.: 7.5 µmol catalyst loading, 40 bar ethylene pressure, 4 hours reaction time, 15 °C reaction temperature, 6.0 g sodium dodecyl sulfate, 1.5 g cesium hydroxide, 0.75 mL mesitylene, in 150 mL degassed water, ultrasound applied prior to ethylene pressurization. [a] given in 10^3 x mol [C_2H_4] x mol^{-1} [Ni]. [b] determined via GPC at 160 °C. [c] determined via DSC, reported as [1st heating cycle (crystallinity) \ 2nd heating cycle (crystallinity)] with 10 K/min heating rate, second line: 1st heating cycle with 1 K/min heating rate. [d] determined via selective detection of methyl and methylene IR-bands during GPC measurements (calibrated versus samples with known degree of branching). [e] determined via DLS, volume mean and PDI reported.

activities (61 x 10^3 TO h^{-1} vs. 73 x 10^3 TO h^{-1}, entries 1 and 2, Table S1); and (3) decreased degrees of branching (1.7 vs. 1.1 branches per 1000 carbon atoms, entries 1 and 2, Table S1) were found. In line with the above polymerizations in heptane and cyclic voltammetry experiments, no significant impact of the longer perfluoroalkyl substituents in catalysts **3-R^F/Pyr** was observed. **3-C$_6$F$_{13}$/Pyr** produce polyethylene with slightly lower activity and, accordingly, with slightly lower molecular weights.

The high functional group tolerance of late transition metal catalysts allows their use even in polar protic environments.[23] During polymerization in aqueous surfactant solution with Ni(II) salicylaldiminato catalysts, the polyethylene is formed in the very unusual form of nanoscale single crystals.[17] They are characterized by a high degree of order, that arises from the unique particle growth mechanism, where the active center's growing chain is directly deposited on the crystal growth front, leaving no opportunity for any disorder.[18,24] This allows for effective generation of anisotropic polymer nanoparticles, that are otherwise difficult to access.[25]

All hydrophilic catalyst precursors of types **1-R^F**, **2-R^F** and **3-R^F** (with H$_2$N-PEG-OMe as labile ligand) were active for several hours under established reaction conditions in water (Table 2). Remarkably, all C$_6$F$_{13}$-substituted catalysts studied are clearly superior in aqueous polymerization compared to their CF$_3$ analogues, in terms of catalytic activity and properties of the produced polyethylenes. In case of catalysts **1-C$_6$F$_{13}$/PEG** and **2-C$_6$F$_{13}$/PEG**, the perfluoroalkyl substitution lead to a comparable substantial increase in catalytic activities (e.g. 23 x 10^3 TO vs. 51 x 10^3 TO, entries 3 and 4, Table 2), molecular weights (408 x 10^3 g mol^{-1} vs. 885 x 10^3 g mol^{-1}, entries 3 and 4, Table 2) and decreased polydispersities (1.8 vs. 1.4, entries 3 and 4, Table 2) and branch contents (1.6 vs. < 1.0 branches per 1000 carbon atoms, entries 1 and 2, Table 2) vs. the trifluoromethyl reference. Under optimized reaction conditions (10 °C reaction temperature, high surfactant loading), both catalysts **1-C$_6$F$_{13}$/PEG** and **2-C$_6$F$_{13}$/PEG** are capable of a truely living ethylene polymerization in water, as evidenced by (1) linear relationships between yields and molecular weights; (2) narrow molecular weight distributions of $M_w/M_n < 1.3$; and (3) chain per nickel ratios close to unity (cf. the SI, Table S2 and S3 for comprehensive experimental and analytical data, and Figure 4). Even linear and narrow distributed UHWMPE with $M_n = 2.0 \times 10^6$ g mol^{-1} is accessible at extended reaction times, as one nickel center grows one polymer chain over the entire polymerization experiment.

Likewise, catalyst **3-C$_6$F$_{13}$/PEG** stands out as the first reported *N*-naphthyl type nickel(II) salicylaldiminato catalyst with adequate activities in water and accessible molecular weights of $M_n = 1.6 \times 10^6$ g mol^{-1} with very narrow distributions of $M_w/M_n = 1.1$, that is formed in a strictly living polymerization (cf. the SI, Table S4 for comprehensive experimental and analytical data, and Figure 4). Different from the non-aqueous polymerization with catalyst motif **3-R^F**, in the aqueous polymerization the CF$_3$ analog is much less active (45 x 10^3 TO vs. 8 x 10^3 TO, entries 5 and 6, Table 2) and less controlled compared to the perfluoroalkyl complex. As polymerizations under aprotic conditions and insights from cyclic voltammetry experiments did not suggest a significant electronic influence of the long perfluoroalkyl groups on the active center for this catalyst type **3-R^F**, we tentatively address this different behavior in the aqueous system to the highly hydrophobic groups on the salicylaldiminato ligand. Possibly, the four C$_6$F$_{13}$-substituents create a highly apolar environment around the metal center, that promotes rapid dissociation of the hydrophilic polar labile H$_2$N-PEG-OMe ligand into the aqueous solution and allows for an effective catalyst activation. ^{1}H-NMR spectra of catalysts **3-R^F/PEG** point to a very strong binding of the labile ligand to the nickel center, as indicated by a hindered rotation (diastereotopic character) of the amino functionality and the protons in α- and β-positions (cf. the SI, Figure S10, S12 and S15), that might prohibit an effective activation in case of the catalyst with exclusively trifluoromethyl substituents.

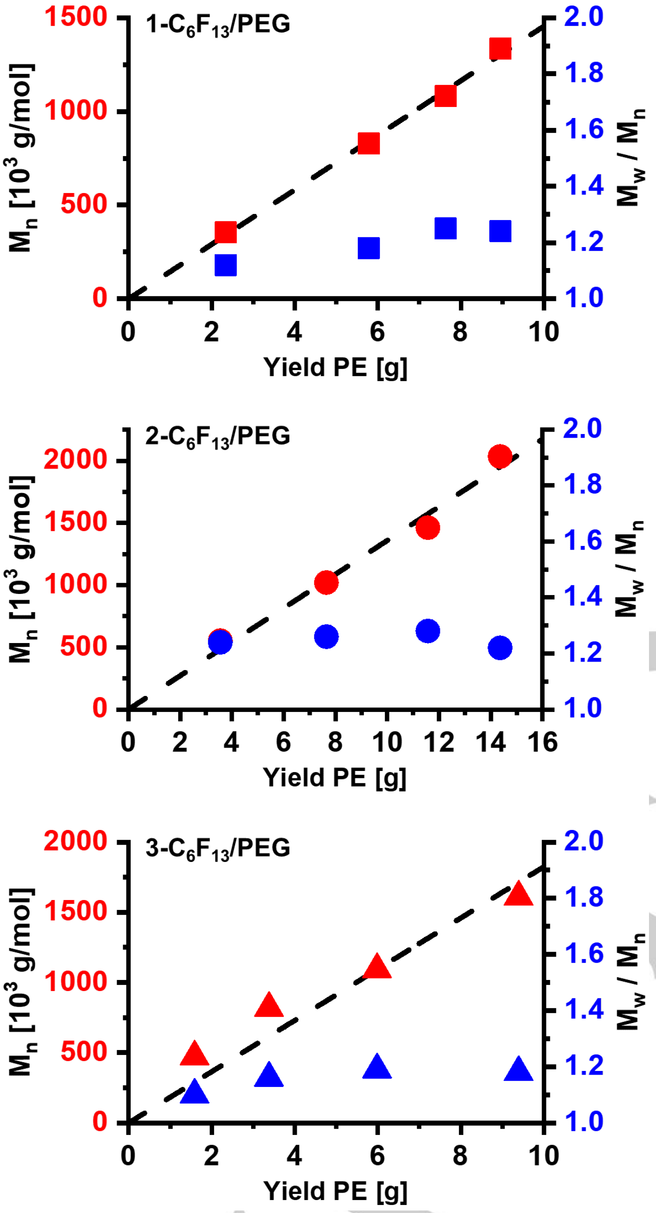

Figure 4. Molecular weights and polydispersity indices of formed polyethylenes versus yields from different aqueous polymerizations with different catalyst precursors (cf. the SI, Tables S2, S3 and S4 for comprehensive experimental and analytical data).

Considering the particle formation process, the generation of very small (<100 nm) particles requires a high degree of dispersion of the catalyst precursor[26], and under ideal conditions an entire particle is grown by a single active site.[10] With the catalysts studied here, stable dispersions with a single well-defined particle population were obtained as observed by DLS (Figure 5). Even these highly fluorinated catalysts (e.g. 36 perfluorinated carbon atoms in chemical structure of **2-C_6F_{13}/PEG**) are able to form small uniform particles under aqueous conditions, which are composed of completely disentangled polyethylene as evidenced by high melting points in the first heating cycle, that are not observed for slow heating rates.[27]

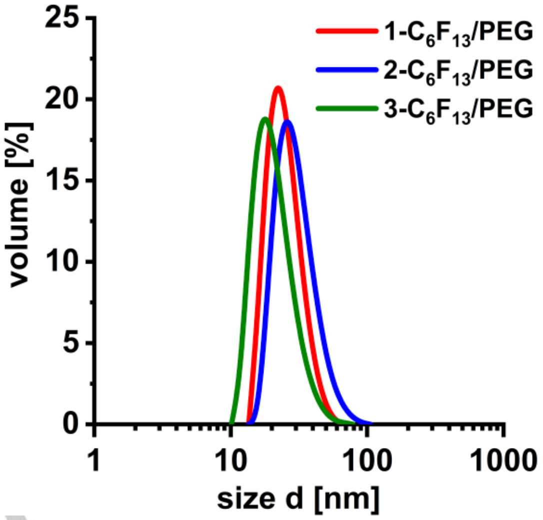

Figure 5. DLS traces of polyethylene dispersions obtained from aqueous polymerization with different catalyst precursors (entries 2,4 and 6, Table 2).

Conclusion

In summary, we present a clear case demonstrating the utility of perfluoroalkyl substituents to control catalytic properties. This demonstrates their potential for catalysis beyond the established use for achieving solubility in very apolar and fluorous media. The C_6F_{13} groups in the catalyst motifs studied substantially increased catalyst activity and molecular weight of the polymer product, and reduced branching. This establishes the mechanistic picture of a reduced electron density on the active metal sites – also supported by cyclic voltammetry on the catalyst precursors – when compared to the more commonly used trifluoromethyl groups. For the catalytic chain growth polymerization studied here, this favors chain growth and disfavors ß-hydride elimination which is the key step of chain transfer and branching pathways. This occurs to an extent that enables truly living polymerizations even in aqueous systems. Perfluoroalkyl groups are similarly or slightly more electron withdrawing compared to CF_3 groups.[28] This accounts for their beneficial impact observed here. Further, longer substituents in the remote positions of the *o*-terphenyl motif also reduce BHE[22], possibly by hindering conformations suitable for an aryl-Ni interaction.

Experimental Section

Experimental Details are described in detail in the Supporting Information.

Acknowledgements

Financial support by the DFG (SFB 1214) is gratefully acknowledged. We thank Anke Friemel for NMR measurements and Sonja Stadler for a sample of **2-CF$_3$/Pyr**. We thank Larissa Casper from Rainer Winters group for support with cyclic voltammetry experiments.

Keywords: aqueous ethylene insertion polymerization • fluorinated ligands • homogeneous catalysis • living polymerization • UHMWPE

---

[1] V. H. Dalvi, P. J. Rossky, *Proc. Natl. Acad. Sci.* **2010**, *107*, 13603–13607.

[2] a) S. Kainz, D. Koch, W. Leitner, W. Baumann, *Angew. Chem. Int. Ed.* **1997**, *36*, 1628–1630; b) Y. Hu, W. Chen, A. M. B. Osuna, J. Xiao, A. M. Stuart, E. G. Hope, *Chem. Commun.* **2001**, 725–726; c) A. Bastero, G. Franciò, W. Leitner, S. Mecking, *Chem. Eur. J.* **2006**, *12*, 6110–6116.

[3] J. A. Gladysz, R. Corrêa da Costa in *Handbook of fluorous chemistry* (Eds.: J. A. Gladysz, D. P. Curran, I. T. Horváth), Wiley-VCH, Weinheim, **2004**, pp. 24–40.

[4] a) S. G. Leach, C. J. Cordier, D. Morton, G. J. McKiernan, S. Warriner, A. Nelson, *J. Org. Chem.* **2008**, *73*, 2753–2759; b) D. Morton, S. Leach, C. Cordier, S. Warriner, A. Nelson, *Angew. Chem. Int. Ed.* **2009**, *48*, 104–109.

[5] a) J. Lim, S. S. Lee, J. Y. Ying, *Chem. Commun.* **2008**, 4312–4314; b) L. V. Dinh, J. A. Gladysz, *Angew. Chem. Int. Ed.* **2005**, *44*, 4095–4097.

[6] a) S. K. Ghosh, A. S. Ojeda, J. Guerrero-Leal, N. Bhuvanesh, J. A. Gladysz, *Inorg. Chem.* **2013**, *52*, 9369–9378; b) Z. Xi, H. S. Bazzi, J. A. Gladysz, *J. Am. Chem. Soc.* **2015**, *137*, 10930–10933.

[7] a) A. R. Ravishankara, S. Solomon, A. A. Turnipseed, R. F. Warren, *Science* **1993**, *259*, 194–199; b) C. C. Tzschucke, C. Markert, H. Glatz, W. Bannwarth, *Angew. Chem. Int. Ed.* **2002**, *41*, 4500–4503; c) M. Wende, R. Meier, J. A. Gladysz, *J. Am. Chem. Soc.* **2001**, *123*, 11490–11491.

[8] a) S. Solyntjes, B. Neumann, H.-G. Stammler, N. Ignat'ev, B. Hoge, *Chem. Eur. J.* **2017**, *23*, 1568–1575; b) R. Mundil, A. Sokolohorskyj, J. Hošek, J. Cvačka, I. Císařová, J. Kvíčala, J. Merna, *Polym. Chem.* **2018**, *9*, 1234–1248; c) H. Jiao, S. Le Stang, T. Soós, R. Meier, K. Kowski, P. Rademacher, L. Jafarpour, J.-B. Hamard, S. P. Nolan, J. A. Gladysz, *J. Am. Chem. Soc.* **2002**, *124*, 1516–1523.

[9] a) H. Mu, L. Pan, D. Song, Y. Li, *Chem. Rev.* **2015**, *115*, 12091–12137; b) C. Chen, *Nat. Rev. Chem.* **2018**, *2*, 6–14.

[10] M. Schnitte, A. Staiger, L. A. Casper, S. Mecking, *Nat. Commun.* **2019**, *10*, 2592.

[11] L. Falivene, T. Wiedemann, I. Göttker-Schnetmann, L. Caporaso, L. Cavallo, S. Mecking, *J. Am. Chem. Soc.* **2018**, *140*, 1305–1312.

[12] M. A. Zuideveld, P. Wehrmann, C. Rohr, S. Mecking, *Angew. Chem. Int. Ed.* **2004**, *43*, 869–873.

[13] I. Göttker-Schnetmann, P. Wehrmann, C. Röhr, S. Mecking, *Organometallics* **2007**, *26*, 2348–2362.

[14] a) H. M. Moeller, M. C. Baier, S. Mecking, E. P. Talsi, K. P. Bryliakov, *Chem. Eur. J.* **2012**, *18*, 848–856; b) M. Mitani, T. Nakano, T. Fujita, *Chem. Eur. J.* **2003**, *9*, 2396–2403.

[15] M. P. Weberski, C. Chen, M. Delferro, C. Zuccaccia, A. Macchioni, T. J. Marks, *Organometallics* **2012**, *31*, 3773–3789.

[16] A. Osichow, I. Göttker-Schnetmann, S. Mecking, *Organometallics* **2013**, *32*, 5239–5242.

[17] I. Göttker-Schnetmann, B. Korthals, S. Mecking, *J. Am. Chem. Soc.* **2006**, *128*, 7708–7709.

[18] A. Osichow, C. Rabe, K. Vogtt, T. Narayanan, L. Harnau, M. Drechsler, M. Ballauff, S. Mecking, *J. Am. Chem. Soc.* **2013**, *135*, 11645–11650.

[19] P. Kenyon, S. Mecking, *J. Am. Chem. Soc.* **2017**, *139*, 13786–13790.

[20] a) P. Kenyon, M. Wörner, S. Mecking, *J. Am. Chem. Soc.* **2018**, *140*, 6685–6689; b) Z. Chen, M. Mesgar, P. S. White, O. Daugulis, M. Brookhart, *ACS Catal.* **2015**, *5*, 631–636.

[21] a) L. K. Johnson, C. M. Killian, M. Brookhart, *J. Am. Chem. Soc.* **1995**, *117*, 6414–6415; b) T. R. Younkin, E. F. Conner, J. I. Henderson, S. K. Friedrich, R. H. Grubbs, D. A. Bansleben, *Science* **2000**, *287*, 460–462.

[22] T. Wiedemann, G. Voit, A. Tchernook, P. Roesle, I. Göttker-Schnetmann, S. Mecking, *J. Am. Chem. Soc.* **2014**, *136*, 2078–2085.

[23] a) A. Nakamura, S. Ito, K. Nozaki, *Chem. Rev.* **2009**, *109*, 5215–5244; b) M. R. Radlauer, A. K. Buckley, L. M. Henling, T. Agapie, *J. Am. Chem. Soc.* **2013**, *135*, 3784–3787.

[24] A. Godin, I. Göttker-Schnetmann, S. Mecking, *Macromolecules* **2016**, *49*, 8825–8837.

[25] a) D. J. Walsh, D. Guironnet, *Proc. Natl. Acad. Sci.* **2019**, *116*, 1538–1542; b) C. E. Boott, J. Gwyther, R. L. Harniman, D. W. Hayward, I. Manners, *Nat. Chem.* **2017**, *9*, 785–792.

[26] C. Boucher-Jacobs, M. Rabnawaz, J. S. Katz, R. Even, D. Guironnet, *Nat. Commun.* **2018**, *9*, 841.

[27] S. Rastogi, D. R. Lippits, G. W. H. Höhne, B. Mezari, C. M. M. Magusin, P., *J. Phys.: Condens. Matter* **2007**, *19*, 205122.

[28] a) C. Hansch, A. Leo, R. W. Taft, *Chem. Rev.* **1991**, *91*, 165–195; b) J. A. Gladysz in *Handbook of fluorous chemistry* (Eds.: J. A. Gladysz, D. P. Curran, I. T. Horváth), Wiley-VCH, Weinheim, **2004**, pp. 41–55.

Entry for the Table of Contents

Layout 1:

RESEARCH ARTICLE

Long perfluoroalkyl substituents in remote positions can influence the active center of nickel(II) salicylaldiminato catalysts to form linear polyethylene of higher molecular weights and in higher activities.

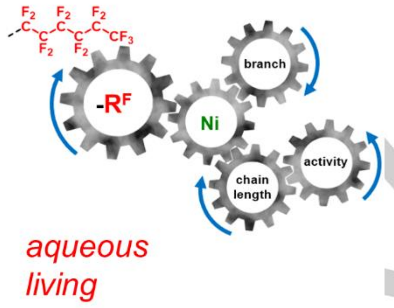

*Manuel Schnitte, Janine S. Scholliers, Kai Riedmiller, S. Mecking**

Page No. – Page No.

Remote Perfluoroalkyl Substituents are Key to Living Aqueous Ethylene Polymerization